Results in Geophysical Sciences 8 (2021) 100030

Contents lists available at ScienceDirect

Results in Geophysical Sciences

journal homepage: www.sciencedirect.com/journal/results-in-geophysical-sciences

Analysis of situ elemental concentration log data for lithology and mineralogy exploration— A case study

Ahmed Amara Konaté [a,*], Houalin Ma [b], Heping Pan [b], Nasir Khan [b]

[a] Laboratoire de Recherche Appliquée en Géoscience et Environnement, Institut Supérieur des Mines et Géologie de Boké, BP: 84, Baralandé, Tamakéné, Boké, Republic of Guinea

[b] Institute of Geophysics and Geomatics, China University of Geosciences (Wuhan), Lumo Road 388, Postal code: 430074, Wuhan, Hubei, China

A R T I C L E I N F O

Keywords:
Metamorphic rocks
Geochemical log interpretation
CCSD-MH
Pearson correlation
Cross plot
Factor analysis

A B S T R A C T

Metamorphic rocks are diverse with more compositions, structures, and textures that are complex. Rock type identification and prediction from metamorphic rocks using well log data are difficult tasks. This study shows the use of cross plot technique, Pearson correlation, and factor analysis in metamorphic rocks interpretation using borehole geochemical data from the 4390–5089 m interval depth of the Chinese Continental Scientific Drilling Main hole. Lithological identification abilities, correlation between geochemical and geophysical logs, and build a factor model which link in situ chemical element to minerals were studied. The results show that Potassium and Thorium logs are the most discriminating logs in metamorphic rocks. Pearson correlation shows that Potassium and Thorium are the largest contributors to the gamma ray responses. Factor analysis results show a 2 factor model-where factor 1 (amphibole mineral) and factor 2 (K-feldspar mineral) described 76.261% of the variation in log responses. These statistical methods can be a very helpful tool in helping the task of geoscientists in the context of research drillings.

Introduction

One of the oldest and most utilized methods that depend on the physical (as well as chemical) properties of rocks is subsurface well logging. Subsurface well logging provides continuous records on the composition and structural features of the penetrated rock. This allows the estimation of lithology and rock properties. As compared to sedimentary rocks, metamorphic rocks are more diverse with more compositions, structures, and textures that are complex. For instance, sedimentary rocks are generally sub-horizontally stratified, dolomites, sandstones and limestones; the boundaries between these strata play as indicator horizons which are readily correlated between wells. However, metamorphic rocks take into consideration a varied range of types from volcanics to massive intrusive rocks of various chemical compositions. Due to their great age and often complicated geologic history, crystalline rocks can be very structurally complex and can be fractured (Monier-Williams et al., 2009). Rock type identification and prediction from metamorphic rocks using well log data are difficult tasks because of their complicated geological characteristics (Mattsson 2007; Maiti et al., 2007; Maiti and Tiwari 2009; Bosch et al., 2013; Luo and Pan 2010; Pan et al., 2010). Knowledge in the use of logging technique in metamorphic rocks has been greatly improved due to scientific research programs such as Forsmark Site(Sweden), KTB (Germany), KOLA (Russia), Cajon Pass (USA), Uveghuta Site(Hungary), Granitic Rock(Czech Republic), Chinese Continental Scientific Drilling (CCSD) (China). The latter is our concern in this study. The CCSD was a joint project by the Chinese government and the International Continental Drilling Program (ICDP). The major scientific goal of CCSD was to access the key composition, deep structure, and active processes of the Sulu UHP metamorphic belt that are not exposed, by means of drilling a hole into the continental crust (Xu et al., 2009). The CCSD-Main Hole (CCSD-MH) is located near Maobei Donghai County, at the Sulu UHP metamorphic belt of Eastern China (Fig. 1). This UHP metamorphic belt is the world's largest and has attracted huge interests from scientist public (He et al., 2008). The CCSD arrived at its target depth of 5158 m with a core recovery rate of 85%(Yang et al., 2006). The 5158 m deep main borehole of the CCSD penetrated five main lithological units: paragneiss, orthogneiss, amphibolite, eclogite, and ultramafic rocks (Luo and Pan 2010). The CCSD-MH in China is the deepest penetration (5158 m) drilled into metamorphic rocks, nevertheless it is shallower than the Germany KTB (9101 m) and Russia Kola (12,000 m) drilled holes respectively (Ji and Xu, 2009); and its crustal geology and lithology differ essentially from those sampled by KTB and Kola drilled holes (Ji and Xu, 2009). Fig. 2

* Corresponding author.
E-mail address: konate77@yahoo.fr (A.A. Konaté).

https://doi.org/10.1016/j.ringps.2021.100030
Received 23 November 2020; Received in revised form 23 August 2021; Accepted 25 September 2021
Available online 26 September 2021

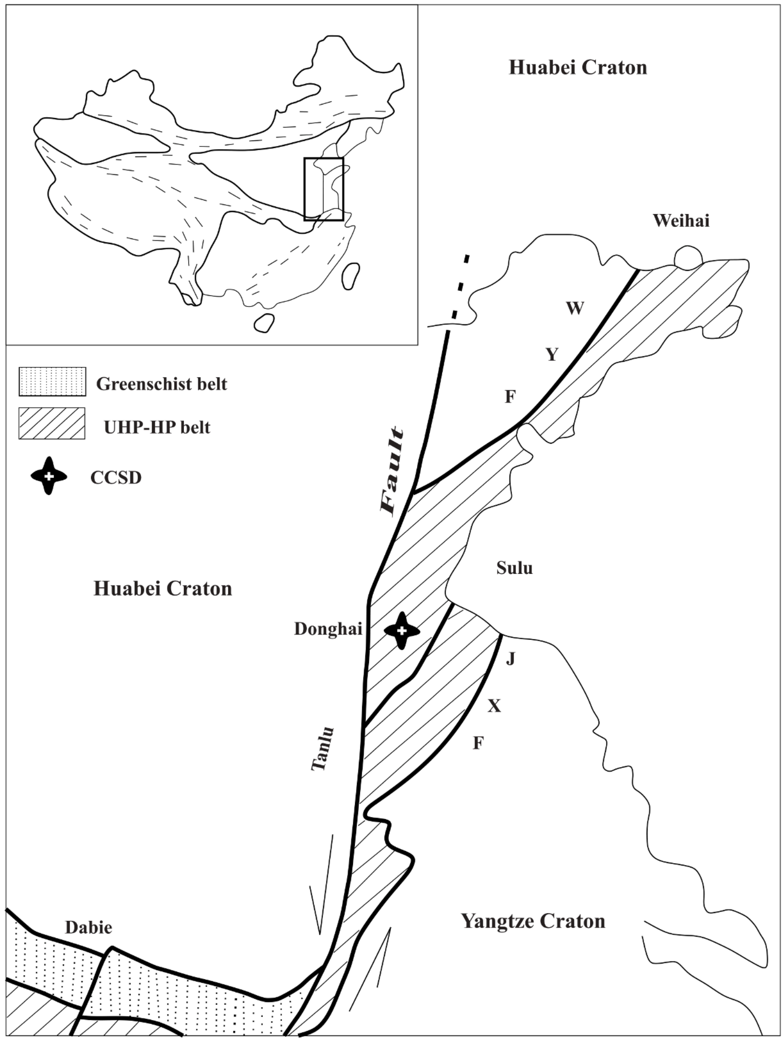

Fig. 1. Location of Chinese Continental Scientific Drilling (CCSD) main hole(after Yang 2009). WYF: Wuliang–Yantai Fault; JXF: Jiashan–Xionshui fault.

illustrated the litho-structural profile of CCSD-MH. More information about the litho-structural of CCSD-MH can be found in (Xu et al., 2009b)).

CCSD-MH was logged immediately after drilling. Geophysical and geochemical logs were run by Shengli Petroleum Logging Company. Geophysical log data has been an important part of research on the UHP metamorphic rocks from CCSD-MH (Pan et al., 2005, 2006; Salim et al., 2008; Luo and Pan 2010; Pan et al., 2010; Luo et al., 2011; Konaté et al. (2015a,b); Yang et al., 2016, 2017). These studies made an important progress in gaining knowledge on the physical properties of different rock type of CCSD-MH. However, effective scientific drilling exploration needs a more ample explanation of the drilled rocks. Consequently, it is vital to investigate of both geochemical and geophysical data to entirely appreciate the log response of CCSD-MH. So in this study, focus is made on geochemical logs analysis.

Geochemical logging provides continuous in situ measurements of the most abundant rock forming and some trace elements (Tamaki et al., 1992). The geochemical log data collected, therefore, offer an alternative possibility for adequate accurate lithology description in both crystalline and sedimentary rocks (Anderson et al., 1988). More details on geochemical logging technique can be found in Hertzog et al. (1989).

It is also important to note the geochemical log data are not widely studied from CCSD-MH. Pan et al. (2010b) and Konaté et al. (2017) investigated on geochemical responses in between 100 and 1000 m and 100- 2010 m depth interval respectively to understand the geochemical properties of rocks. Even though these studies exist, so far the CCSD-MH geochemical data has not yet been totally studied. Therefore, it offers a unique opportunity to study metamorphic rocks log responses of the Sulu UHP metamorphic belt.

The purpose of this study is to analyze the geochemical log responses from CCSD-MH (4390–5089 m). To do so, (1) we analyzed and discussed the abilities of lithological identification using cross plot; (2) we investigated the correlation between geochemical –geophysical logs; and (3) we applied factor analysis to construct a model linking elemental concentration logs to mineral abundances.

The idea behind this study is to evaluate the capabilities of the existing methods in the context of metamorphic rocks especially in the case of the CCSD-MH data. The results show that geochemical data offer adequate evidence for accurate lithological description in metamorphic rocks, and they are an excellent complement to geophysical logging, and core analyses in the studies of the CCSD-MH data. Statistical methods can

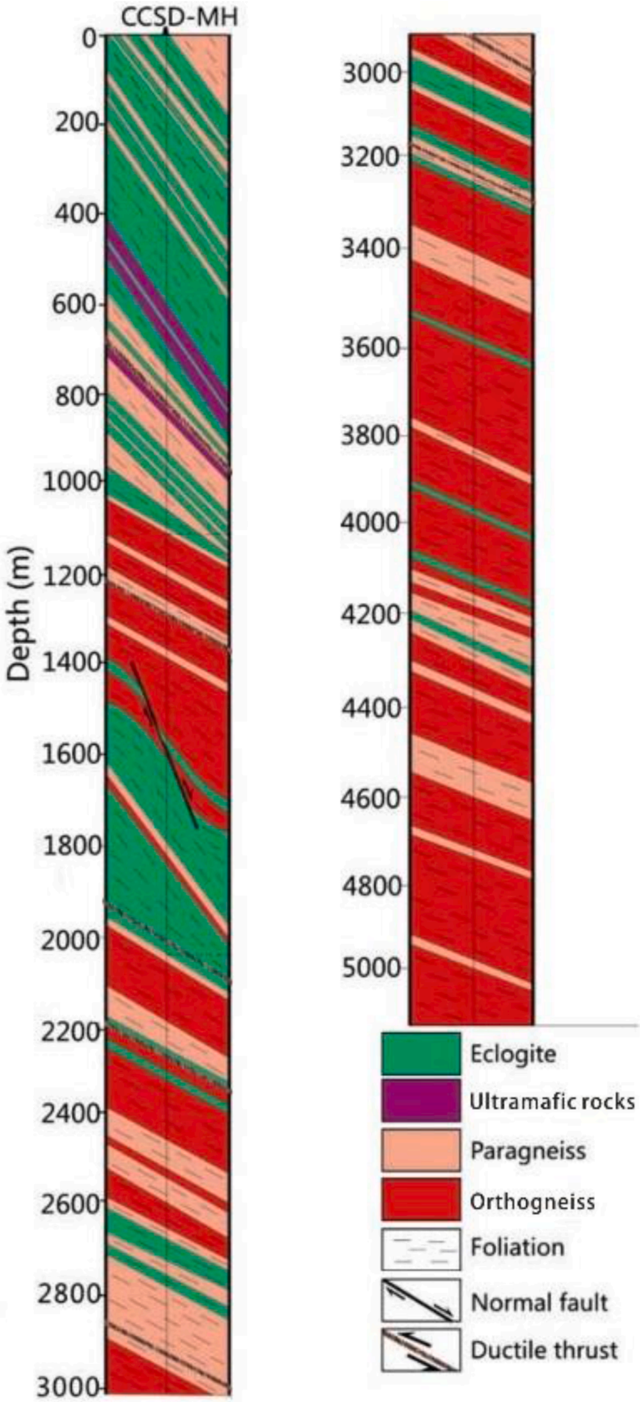

Fig. 2. Simplified litho-structural profile of CCSD-MH (after Xu et al. (2009)).

be a very helpful tool in helping the task of geoscientists in the context of research drillings.

Geological setting of study area

One of the most significant solid earth discoveries of the last three decades is the identification of a large UHP metamorphic belt, more than 1000 km long, in the Sulu–Dabie region of central eastern China (Xu et al., 2009). This UHP metamorphic belt was first subducted into the mantle, and then quickly exhumed back up to the upper crust, producing the largest UHP metamorphic terrane in the world (Yang, 2009 and references therein). The rocks on the surface outcrops in Dabie–Sulu are largely gneisses, comprising monzonitic gneiss, biotite gneiss and biotite plagioclase gneiss. These gneisses were formed in the Proterozoic or older, and underwent UHP metamorphic in the Triassic period; therefore the gneisses exposed on the CCSD site often contain coesite (Yang, 2009 and references therein). The CCSD-MH is located in the sigmoid-shaped Maobei eclogite/ultramafic complex in the northern Sulu UHP upper tectonic slice (Xu et al., 2009). Both coesite and diamond have been discovered in eclogite, and coesite has also been found in orthogneiss, paragneiss, quartzite and marble in the UHP metamorphic belt (Xu et al., 1992, 2009 and references therein). The Sulu–Dabie UHP metamorphic belt located at the east part of the Tanlu fault, resulted from the continental subduction and collision between the North China and the Yangtze cratons during the Triassic (Liu et al., 2010).Referring to Yang (2009), before the collision, the Dabie–Sulu terranes were located in the northern boundary of the Yangtze craton. Nevertheless, they were divided later by the Tanlu fault and the Sulu terrane was displaced in a north direction. Extensive dynamic activity continued after the Triassic collision between the North China and Yangtze cratons. Note that the exhumation of the UHP metamorphic and HP metamorphic rocks, the intracontinental subduction of the Yangtze craton beneath the Sulu and North China craton took place during the early Jurassic. This subduction caused in part of the continental crust subsiding into the upper mantle. Beginning the middle Jurassic, large-scale granitoid intrusions established nearby the Dabie–Sulu zones and other parts of eastern China, probably ensuing from lithospheric thinning and heat flow upwelling from the asthenosphere. The granitic intrusions were followed by rifting and eruption of basalts alone the Tanlu fault zone. The mountain root that existed in the Dabie–Sulu orogenic belt was almost eroded.

The Sulu terrane comprises of a series of HP and UHP metamorphic slices divided by wide shear zones. According to (Xu et al., 2009b) there are four tectonometamorphic zones are with respect to increasing metamorphic grades (Fig. 3).

The Zone I is characterized by low-temperature (LT) and HP zone where glaucophane and kyanite-bearing paragneisses, quartzites and marbles experienced blueschist facies metamorphism at 0.7–0.85 GPa and 300–360 °C. The Zone II is called medium temperature (MT) and very high pressure (VHP) zone which occurred hydroxyl-rich topaz in kyanite quartzites, suggesting the metamorphism at 1.5–2.5 GPa and 500–600 °C. The Zone III is mainly composed of coesite-bearing supracrustal gneisses, quartzites, mica schists and amphibolites. The Zone IV is characterized by granitic gneisses and has been intensely modified by Cretaceous migmatization and granitic plutons. Eclogites and garnet peridotites appear as lenses, pods or layers ranging from tens of centimetres to a few kilometres in size within supracrustal and granitic gneisses in the zones III and IV. The highest metamorphism at 4–7 GPa and 760–970 °C was known in eclogites and garnet peridotites, inferring very low geothermal gradients in a cold subduction zone (Xu et al., 2009b).

Data

This study focuses on the 4390–5089 m depth interval of CCSD-MH, from which 5599 data points were obtained. In this interval, the main lithology is orthogneiss, paragneiss, and amphibolite. Fig. 4. displays the geochemical logs profile of the CCSD-MH (4390–5089 m). The analysis of log data to characterize the lithology requires an increased level of interpretive care and skill. A combined analysis of these logs through

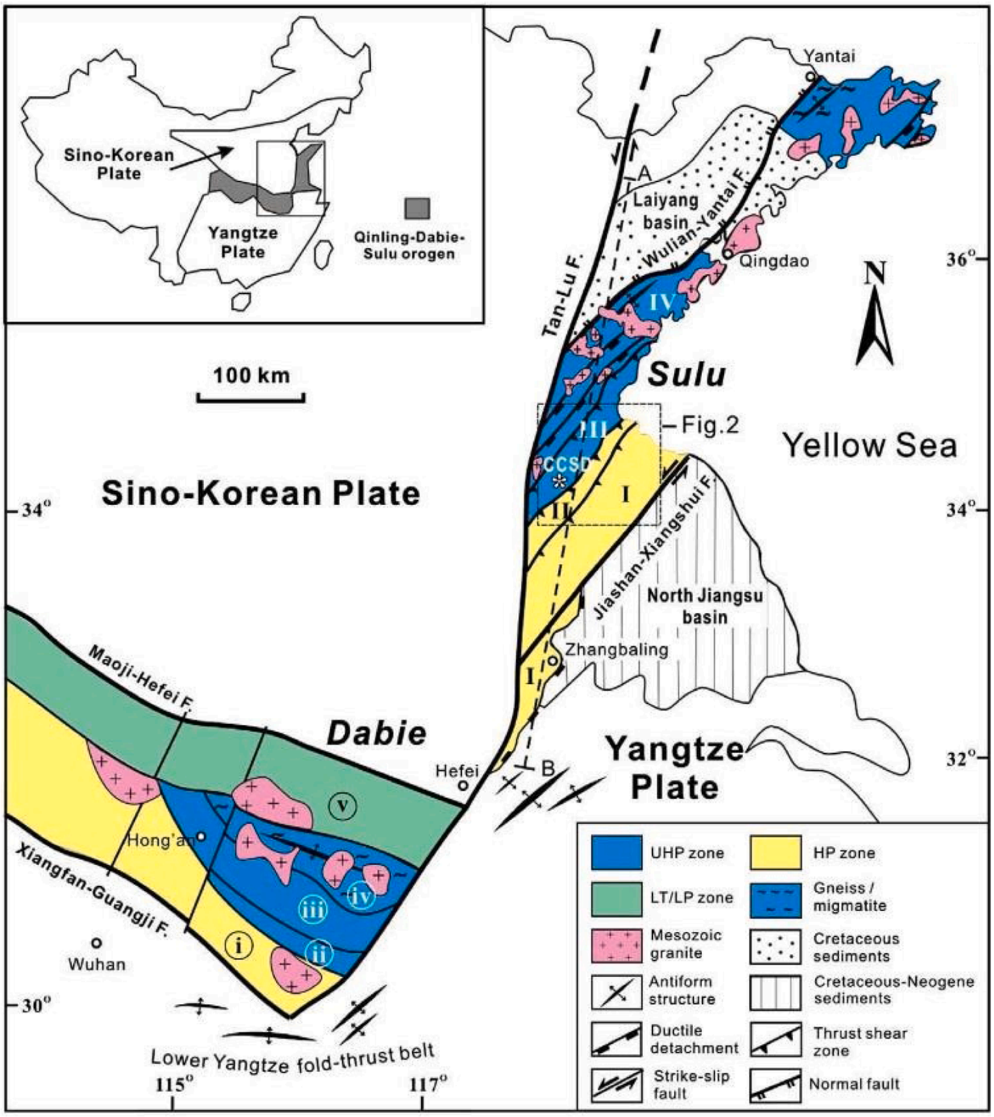

Fig. 3. Geological map of Dabie-Sulu oregen in east central China (after (Xu et al., 2009b)).

statistical approach may improve remarkable diagnostic strength for lithological understanding in the study area. As research on the CCSD project data continues, many new conclusions are expected.

Methods

Cross plot

A graph of two log responses compared to another is called a cross-plot. Two well logs can be cross plotted with one another; at each point in coordinate system corresponding to a measured pair of values defined by the N values of its samples. Proximity of points in the cross plot indicates similar log response. In contrast, separation of points suggests different log response. In this way, the cross plot in the cross plot logs can be viewed as statistical electrofacies as introduced by Serra (1984). Cross plot technique has been, and continue to be, used extensively to identify lithology. Several studies undertaken in Pan et al. (2010); Luo and Pan (2010), Rafik and Kamel, 2016; Das and Chatterjee (2018), Gogoi and Chatterjee (2020) have shown that cross plot have the latent for extracting information from well log curves. Cross plot allows the well log interpreter to visualize the data more successfully than observing at each log individually. Despite its wide-scale usage, however, it has some limitations. Cross plot is multitrack log display become time consuming when the number of logs to be analyzed simultaneously increases (Saggaf and Nebrija 2000). Additionally, this method may generate multiple interpretations because cross plot log interpretation depends on the skill of the log interpreter. More details about this method can be found in Fertl (1981).

Pearson's correlation coefficient

The correlation coefficient was invented by Pearson (1896). A Pearson's correlation coefficient is commonly applied in geoscience to calculate a relationship between two variables. There has been an effort to apply Pearson's correlation coefficient on geophysical log data (Bartetzko et al., 2005; Rafik and Kamel, 2016; Konaté et al., 2017;

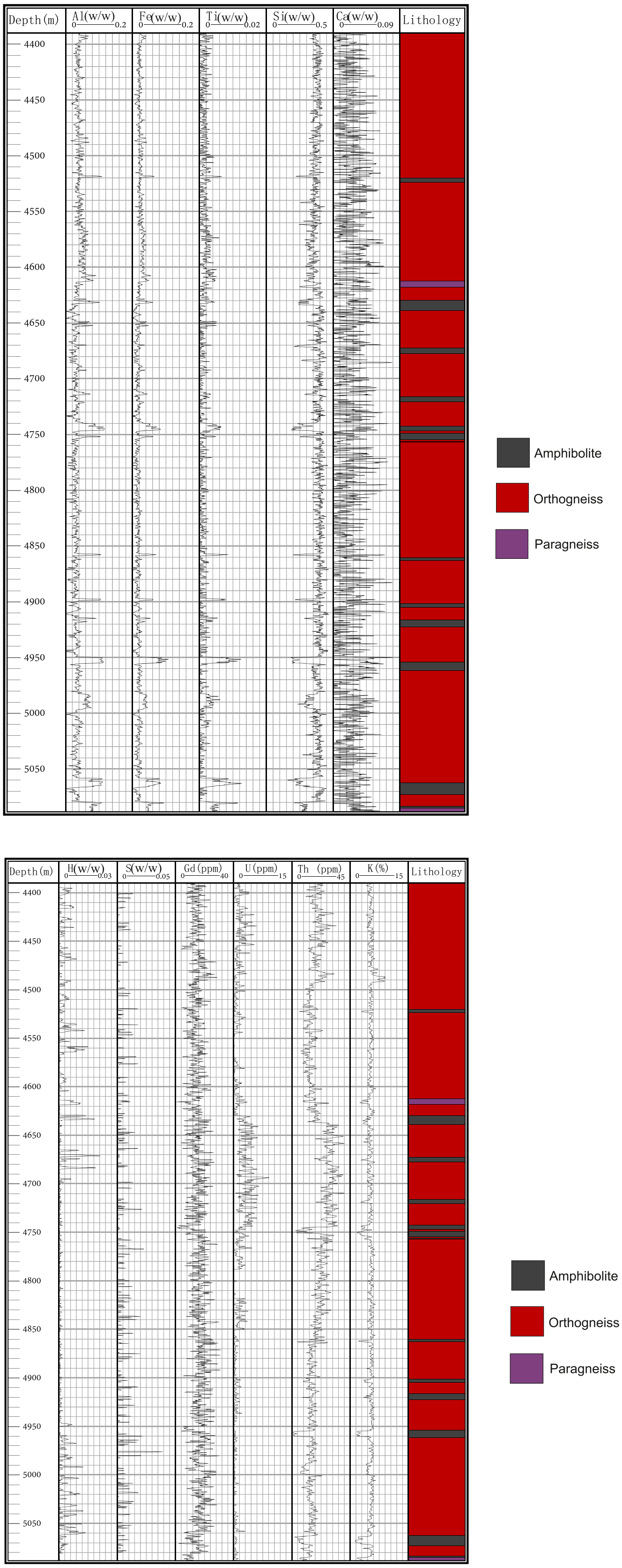

Fig. 4. The geochemical logs (K, Th, Al, Fe, Ti, Si, Ca, H, S, Gd, U, Th, K) profile of the CCSD-MH (4390–5089 m).

Campos da Purificacao and Nery, 2017) Here, it is utilized to determine significant relationship between rock composition and conventional log readings.

The correlation coefficient between two variables **x** and **y** is designated ***rxy***. It can be calculated as:

$$rxy = \frac{cov(x, y)}{\sqrt{var(x)}\sqrt{var(y)}}$$

Where cov(x, y) is covariance of **x** and **y**; var(x) is the sample variance of **x**; var(y) is the sample variance of **y**.

Pearson's correlation coefficient can take on any value in between −1 and 1. The correlation coefficient sign shows the direction of the relationship, whereas the correlation magnitude that is how close it is to −1 or +1 point out the strength of the relationship.

Factor analysis (FA)

Factor Analysis (FA) (Thurstone, 1931) is a statistical approach that tries to detect underlying variables (factors) that explain the pattern of correlations within a set of observed variables. There has been widespread application of FA using well log data (Herron 1986; Bücker et al., 2000; Gelfort 2006; Szabó et al. 2011; Rafik and Kamel 2016). FA is frequently utilized in data reduction to detect a fewer number of factors that explain most of the variance observed in a much larger number of manifest variables. In this research it is supposed that the factors extracted by FA may be connected to the minerals that make up the rock in CCSD-MH (4390–5089 m).

Referring to Rencher (2002), FA aims to reduce the redundancy among the variables by using a smaller number of factors. FA assumes that there is a set of latent factors f_k which when acting in combination to generate the original variables x.

Algebraically, in factor analysis the variables $x_1, x_2, \ldots, x_p$ are represented as linear combinations of a few variables $f_1, f_2, \ldots, f_k$ $(k < p)$ called *factors*. The factors are underlying *constructs* or *latent* variables that "generate" the x's (Rencher, 2002).

Without loss of generality, we assume that $E[x] = 0$. Therefore, the factor analysis model for $k < p$ common factors f_k can be written as follows (Rencher, 2002):

$$x_i = v_{i1}f_1 + v_{i2}f_2 + \ldots + v_{ik}f_k + \varepsilon_i \tag{1}$$

Where the v_{ij} $j = 1,\ldots m$ are the factor loadings (or scores) and ε_i is the part of variable x_i that cannot be 'explained' by the factors.

Equation (3.21) can be written in matrix notation as

$$x = Vf + \varepsilon \tag{2}$$

f= matrix of new variable also called the latent variables in terms of $k \times n$; V= the loading matrix in term of $k \times p$ and x = observation matrix in $p \times n$.

The emphasis in factor analysis is on modeling the covariance or correlations among the x's.

It is assumed that

$$E[f_k] = 0;\ \mathrm{var}(f_k) = I \tag{3}$$

$$E[\varepsilon_i] = 0;\ \mathrm{cov}(\varepsilon_i, \varepsilon_j) = 0\ i \neq j \tag{4}$$

$$\mathrm{cov}(\varepsilon_i, f_k) = 0 \tag{5}$$

Any solution of the above constraints for f is denoted as the factors, and V as the loading matrix.

Variance x may be write as

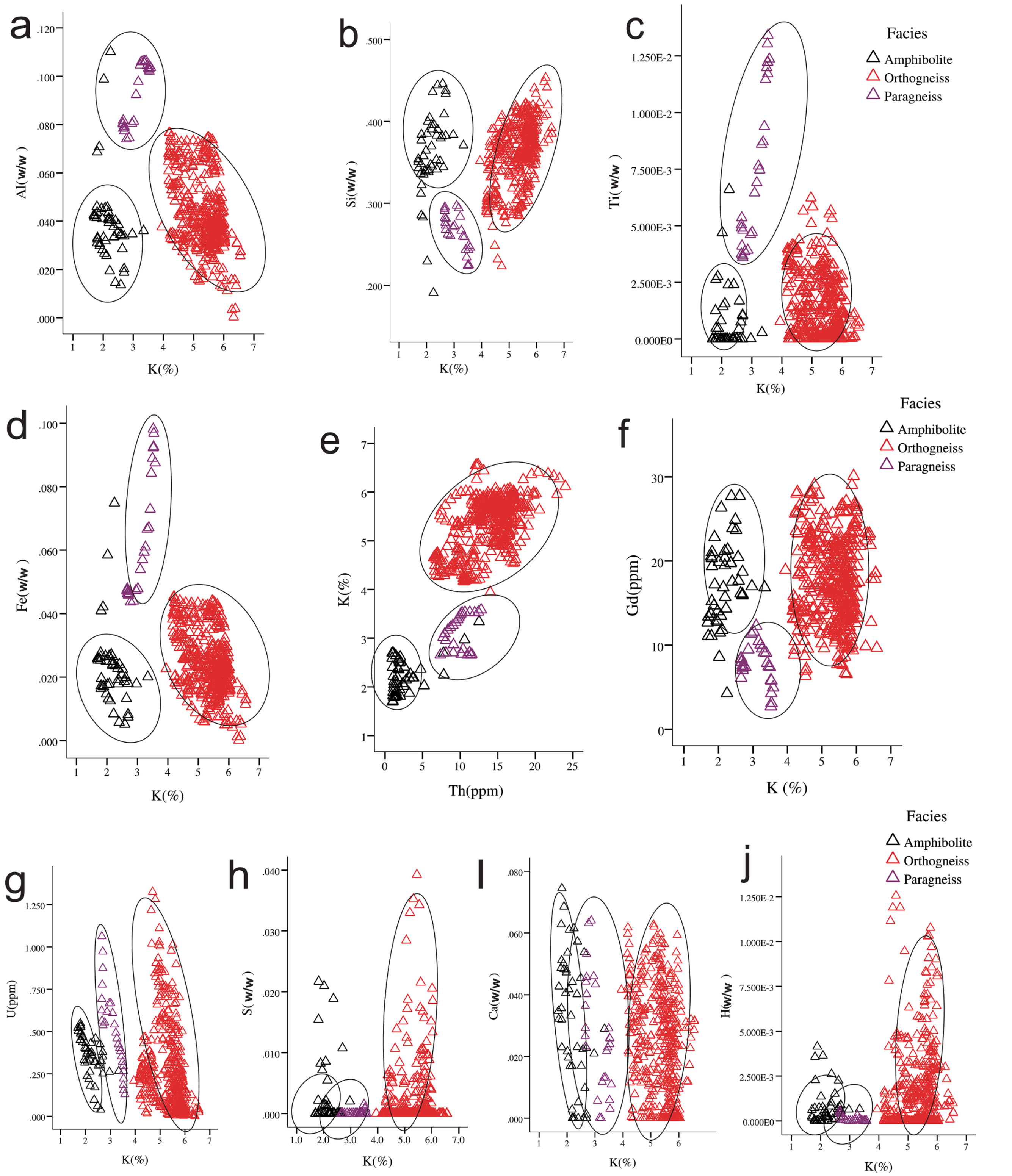

Fig. 5. The cross plots of K against Al, Fe, Si, Ti, Gd, Th, H, S, Ca and U logs respectively.

$$\mathrm{var}(x_i) = \sum_{k=1}^{K} v_{ik}^2 \mathrm{var}(f_k) + \mathrm{var}(\varepsilon_i) \tag{6}$$

Because of $\mathrm{var}(f_k) = I$ and $\mathrm{var}(\varepsilon_i) = \psi_i$

$$\mathrm{var}(x_i) = \sum_{k=1}^{K} v_{ik}^2 + \psi_i \tag{7}$$

$\sum_{k=1}^{K} v_{ik}^2$ is the variance explained by the common factors, called the communality and represents the variance of x_i common to all variables. The term v_{ik}^2 measures the magnitude of the dependence of x_i on the common factor f_k. If several variables x_i have high loadings v_{ik} on a given factor f_k, the implication is that those variables measure the same unobservable quantity, and are therefore redundant. While the second part (ψ_i) is the variance specific to x_i called the specific or unique variance

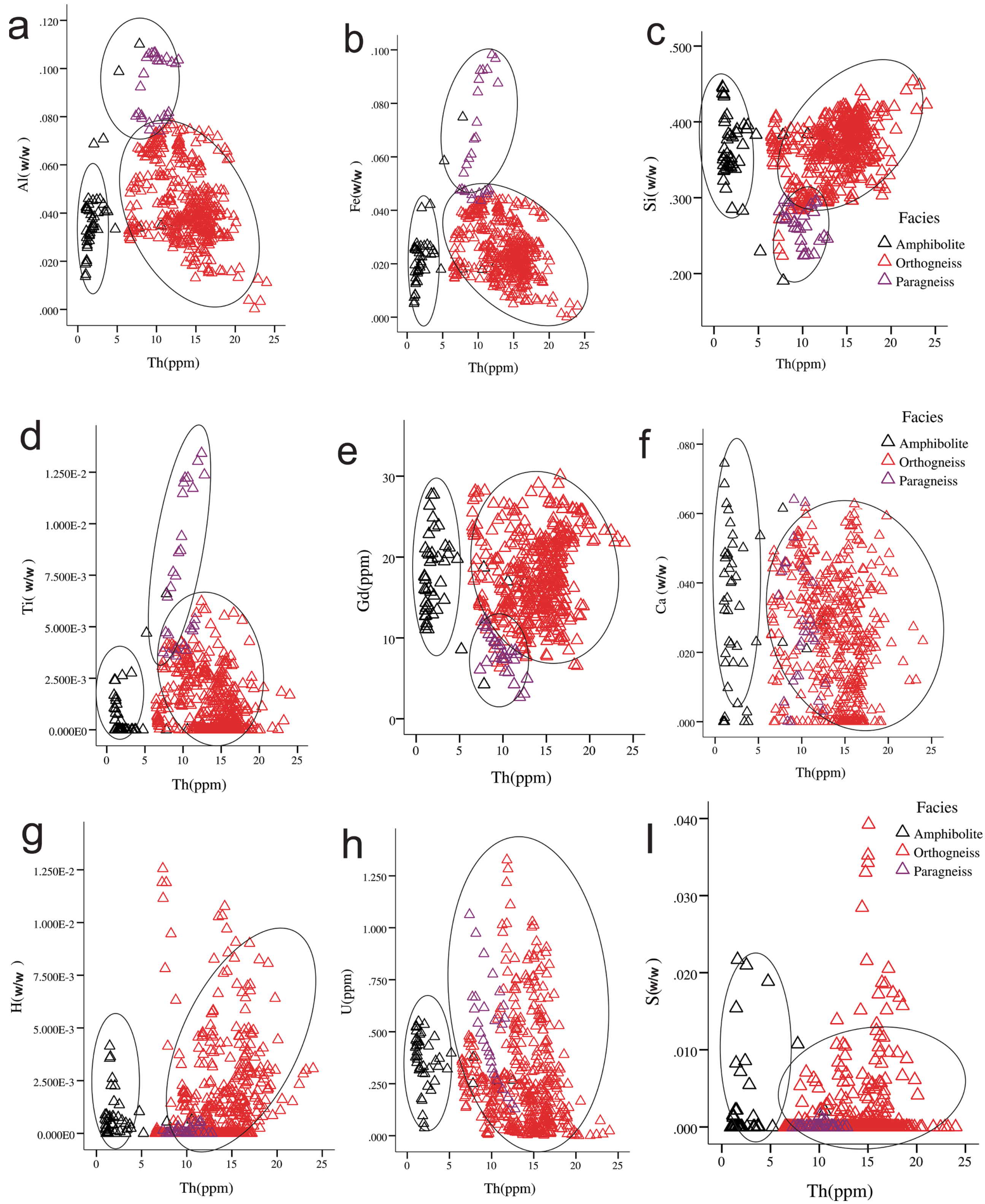

Fig. 6. The cross plots of log Th against Al, Fe, Si, Ti, Gd, H, S, Ca and U log respectively.

and it is the contribution in the variability of x_i due to its specific ε_i part, not shared by the other variables.

So factor analysis is really a model for the covariance matrix Z of the data as

$$\begin{aligned} \mathrm{cov}(x) &= \mathrm{cov}(Vf + \varepsilon) \\ &= \mathrm{cov}(Vf) + \mathrm{cov}(\varepsilon) \\ &= V\mathrm{cov}(f)V^T + \Psi \end{aligned} \quad (8)$$

Because of $\mathrm{cov}(f) = I$, then we get

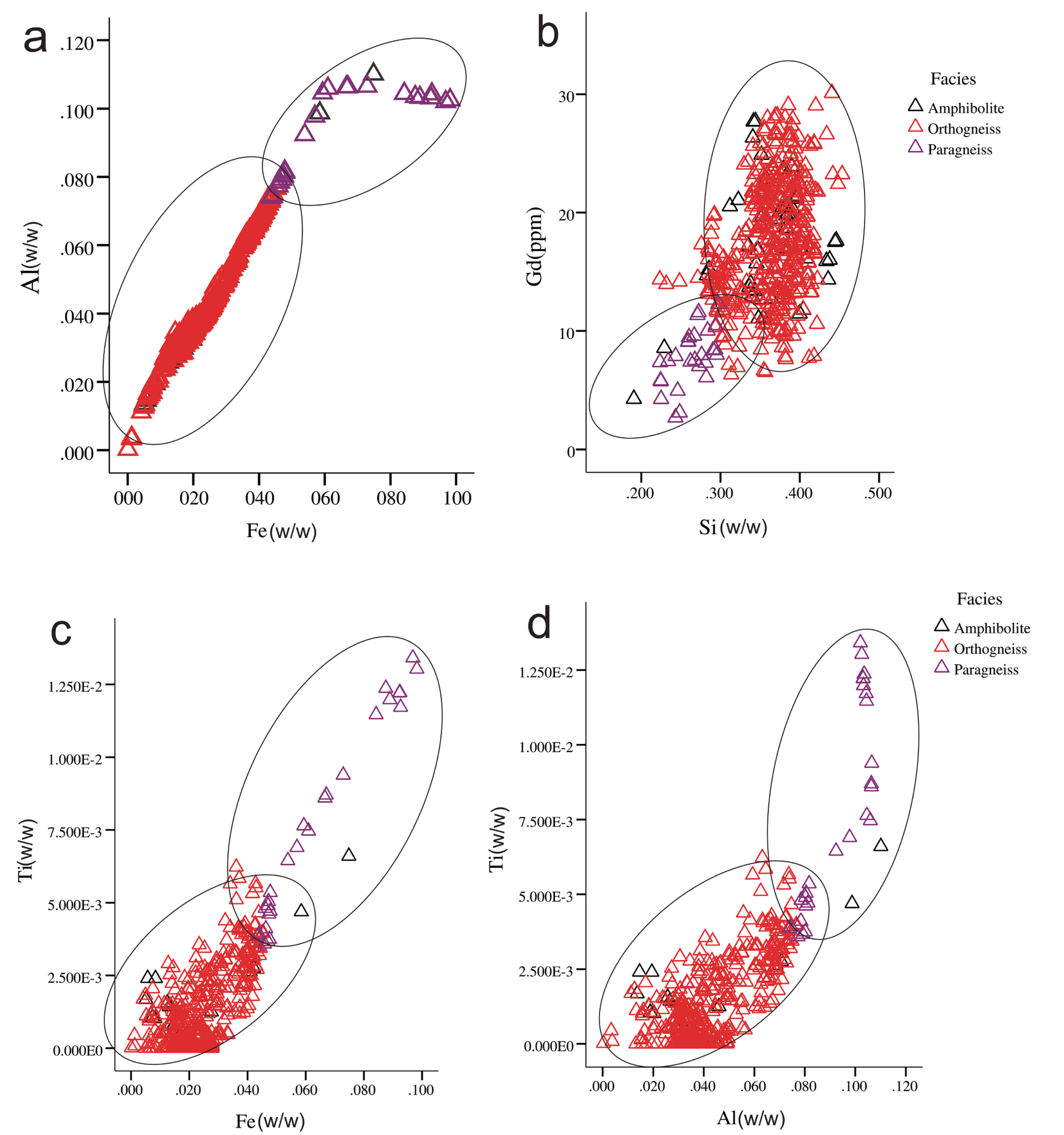

Fig. 7. a-d. Cross plotting of geochemical logs. (a) Cross plot of Fe versus Al. (b) Cross plot of Si versus Gd. (c) Cross plot of Fe versus Ti. (d) Cross plot of Al versus Ti.

$$VV^T + \Psi \tag{9}$$

Where $\Psi = diag(\psi_{11}, \psi_{22}, ..., \psi_{pp})$

Given Z as the estimator of cov(x), we want to find V and Ψsuch that $Z = VV^T + \Psi$ (3.30 10)

It is important to note that if there are only a few factors (i.e., $k << p$), then we can get a simplified structure for Z. There are different methods such as principal component, maximum likelihood, and principal axis factoring and rotation to derive estimates V and Ψ for the model parameters in Eqs. (2)-(5).

FA is related to Principal Component Analysis (PCA) in that both seek a simpler structure in a set of variables but they differ in many respects. For example, two differences in basic approach are as follows (Rencher, 2002): PCs are defined as linear combinations of the original variables, while FA, the original variables are expressed as linear combinations of the factors. In PCA, we explain a large part of the total variance of the

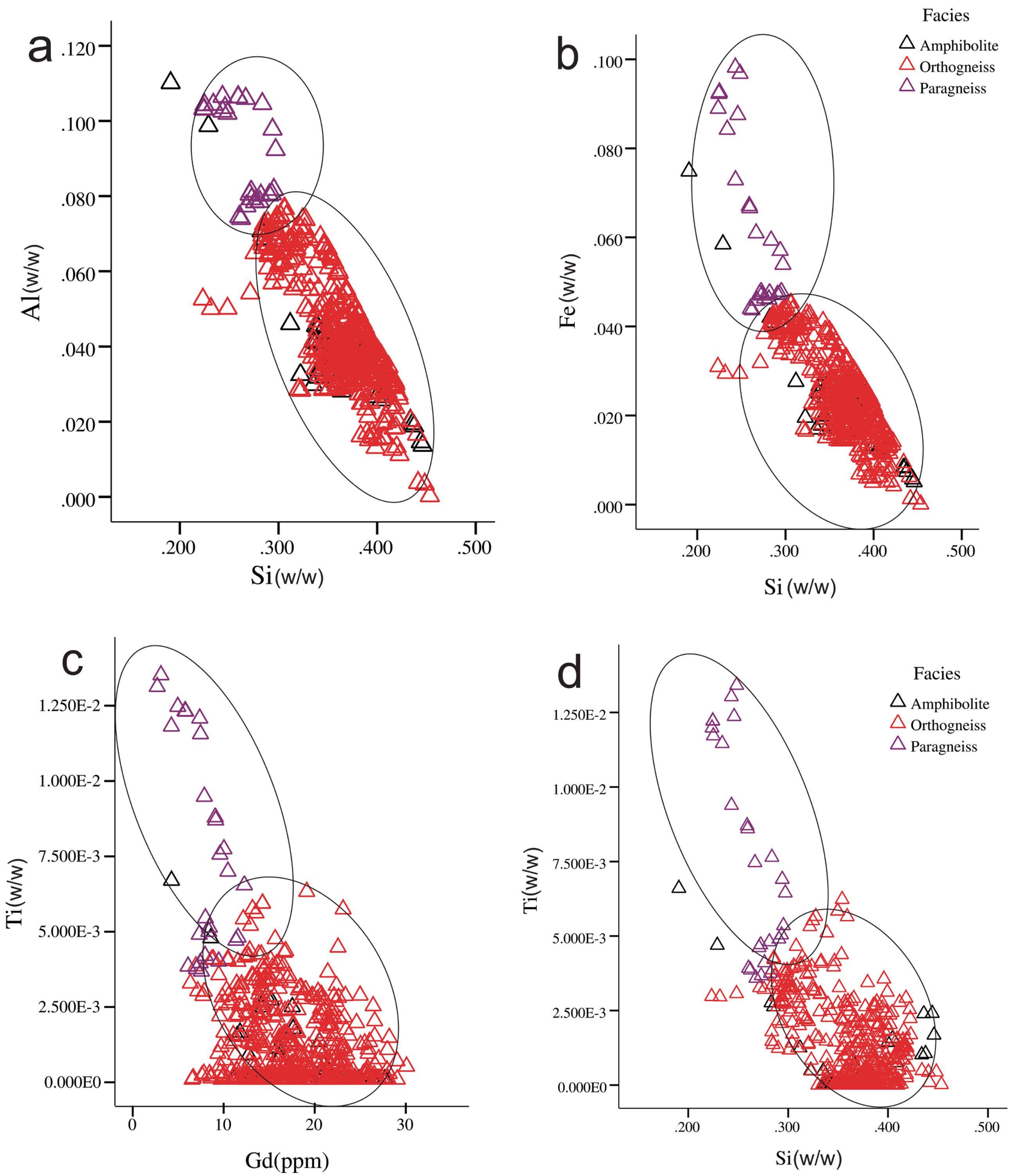

Fig. 8. a-d. Cross plotting of geochemical logs. (a) Cross plot of Si versus Al. (b) Cross plot of Si versus Fe. (c) Cross plot of Gd versus Ti. (d) Cross plot of Si versus Ti.

variables, in contrast FA seek to account for the covariance or correlations among the variables.

Results and discussions

Lithological identification- cross -plots

Cross plots were utilized to examine the relationship between log type responses in order to understand the rock types from CCSD-MH. From Fig. 5.a-j, data grouping is well discernible in Fig. 5.a-f and the lithologies are well separated. In Fig. 5.g-j, discriminations of rock types are not as clearly evident as in Fig. 5.a-f. This is for the reason that the data are dispersed or lithologies are skewed by very low values and there are reasonably overlaps between lithologies. Therefore, the cross plot of K against Al, Fe, Si, Ti, Gd and Th logs are appropriate for separating metamorphic rocks. This fact is associated to K. Comparable performance of K is also visible in Konaté et al.(2015b, 2017); by inspecting the cross- plot log response of various geophysical logs, and geochemical

Table 1

The log values statistics for the metamorphic rock types from CCSD-MH (4390–5089 m). The minimum, maximum, means values and standard deviation are showed for each electrofacies. An electrofacies characterizes a rock type by a specific set of log responses. By using core-log-correlation, the geochemical log data were allocated to the different metamorphic rock types (Serra 1984). From Table 1, the average K values of the orthogneisses are about 5.315% while for paragneisses and amphibolites are about 3.021% and 2.757% respectively. Intermediate Th value occurs in orthogneisses, with about 19.131 ppm. Besides the paragneisses and amphibolites have lower Th values as compared to orthogneisses rocks. Similar performance is achieved by Gd. The average U of orthogneisses, paragneisses and amphibolite are 1.225±1.416 ppm, 1.077±1.093 ppm and 0.860±0.836 ppm respectively. The Al average values of orthogneisses, paragneisses and amphibolite are (0.038±0.016 w/w), (0.080±0.024 w/w) and (0.044±0.030 w/w) respectively. Orthogneisses and amphibolites are in similar ranges. Similar performance is made by Ti, Fe and Si.

		Gadolinium (ppm)				Iron (w/w)				Silicon (w/w)			
Lithology	N	Min	Max	Mean	Std.Dev.	Min	Max	Mean	Std.Dev.	Min	Max	Mean	Std.Dev.
Orthogneisses	5348	0.891	31.396	15.658	4.511	0.000	0.106	0.021	0.012	0.154	0.467	0.373	0.043
Amphibolites	216	0.275	27.710	13.806	5.742	0.000	0.083	0.025	0.021	0.181	0.452	0.361	0.069
Paragneisses	35	2.695	12.275	7.822	2.258	0.016	0.098	0.055	0.024	0.223	0.373	0.282	0.044
		Aluminum (w/w)				**Titanium (w/w)**				**Potassium (%)**			
Lithology	**N**	Min	Max	Mean	Std.Dev.	**Min**	**Max**	**Mean**	**Std.Dev.**	**Min**	**Max**	**Mean**	**Std.Dev.**
Orthogneisses	5348	0.000	0.114	0.038	0.016	0.000	0.012	0.001	0.000	2.307	9.132	5.315	0.614
Amphibolites	216	0.000	0.116	0.044	0.030	0.000	0.009	0.001	0.002	1.244	5.825	2.757	0.947
Paragneisses	35	0.027	0.106	0.080	0.024	0.001	0.013	0.006	0.003	2.519	3.582	3.021	0.371
		Thorium(ppm)				**Uranimum (ppm)**							
Lithology	**N**	**Min**	**Max**	**Mean**	**Std.Dev.**	**Min**	**Max**	**Mean**	**Std.Dev.**				
Orthogneisses	5348	2.845	40.709	19.131	6.478	0	9.156	1.225	1.416				
Amphibolites	216	0.954	26.250	7.908	5.462	0.014	4.861	0.860	0.836				
Paragneisses	35	7.370	25.848	11.328	3.756	0.129	3.509	1.077	1.093				

logs respectively. Pan et al. (2005) based on cross plotting logging interpretation to make estimates of lithology.The authors' conclusion was that the different rock types in the CCSD-MH can be well recognized using K against various geophysical logs such as density (DEN), natural gamma (GR), neutron porosity (CNL), the photoelectric absorption section index (PE) and resistivity logs. On the other hand, Salim et al. (2008) also used cross plotting technique to define lithological units of different rock units. They reported that GR is positively correlated to K (as well as Th, U content), and GR (as well as K, Th, U content) and DEN are efficient to discriminate metamorphic rocks. Luo and Pan (2010) used cross plotted conventional logs data, and the results allowed the authors to conclude that the lithology principally consists of paragneiss, orthogneiss, amphibolite, eclogite and ultramafic rocks. The logs cross plotting show that K and CNL are more prevailing in identifying metamorphic rocks. Furthermore, the work of Pechnig et al. (2005) from several drilled well in continental crust, confirmed that K and CNL are more powerful in discriminating metamorphic rock type. Based on the aforementioned results, we can say that K is a key factor of lithological identification in metamorphic rocks. In an environment underlain by crystalline rocks, metamorphism plays an important part in producing changing mineral composition and structural variations of crystalline rocks (Maiti and Tiwari, 2009). K is movable throughout alteration and metamorphism process (Bartetzko et al., 2005). So K enrichment in the CCSD-MH is perhaps associated with UHP metamorphism.

From Fig. 6.a-e, we can see that the cross plot of Th against Al, Fe, Si, and Ti are appropriate for discriminating between the rock types. However, the discriminations of the rock types are not as evidently distinct as Fig. 6.a-f. This is because orthogneiss is slightly scattered and coincide partially with paragneiss. In Fig. 6.f-i, the data are extensively scattered and there are solid overlaps between rock types. Paragneiss and orthogneiss cannot be distinguished. Hence, Th is not as powerful as K. Th has low mobility under metamorphism as compared to K. Cross plot of the positive correlation between K and Th (see Fig. 5.e) shows that, from amphibolites to orthogneisses, the intensity of K and Th is gradually increasing. So intermediate-high K and Th indicate the presence of orthogneisses. This is consistent with Liu et al. (2005) which analyzed cores from CCSD-MH and concluded that orthogneisses are relatively enriched in K and Th. Additionally, the study of Salim et al. (2008) confirmed the positive correlation between K and Th content, and showed that K and Th content of gneiss is high.

From Figs. 7.a-d and 8.a-d, we can observe that orthogneisses widely lie over amphibolites because the log signatures of these rocks are similar. This can be additionally seen in Table 1. However paragneisses are separated from orthogneisses/amphibolites. The cross plots of log Fe versus Al and Ti (see Fig. 7.a and c) show positive trend from orthogneisses/amphibolites to paragneisses .This trend is related to the elemental concentration variability that is Fe increase with increasing of Al and Ti respectively. However an opposite trend is observed in the cross plots of Si versus Al, Fe and Ti respectively (Fig. 8.a-b and d). Similar opposite trend is observed in the cross plot of log Ti versus Gd (Fig. 8.c). Therefore Al, Fe, Si and Ti, Gd logs are helpful in distinguishing amphibolites from paragneisses, and paragneisses from orthogneisses on the other hand.

By analyzing the above development, we can conclude that K and Th logs are the most discriminating logs in UHPM rocks followed by the Ti, Al, Fe, Si and Gd logs. Table 1 shows the log values statistics for the metamorphic rock types from CCSD-MH (4390-5089 m).

In situ geochemical –geophysical log relationship

Geochemical logs and geophysical logs were compared in order to determine significant relationship between rock composition and log readings. This objective was reached using the Pearson correlation coefficient. The results are presented in Table 2. Fig. 9 shows the geophysical logs profile of the CCSD-MH (4390–5089 m). In Table 2, the GR shows important positive correlation with K and Th respectively. So Th and K are the largest contributors to the gamma ray responses in the UHP metamorphic rocks from CCSD-MH. This assertion has confirmed by Salim et al. (2008).The authors showed that K and Th content of metamorphic rocks shows positive correlation with GR responses respectively. Again, in Table 2 there is no important correlation between CNL and H. This is not surprising, as the CNL logging tool cannot be used as a measure of formation porosity in crystalline rocks (Bartetzko et al., 2005).The CNL tool measures the formation porosity according to the hydrogen content in the formation. Resistivity and acoustic logs display no significant relationship with any of the geochemical logs in Table 2. This can be additionally view in Figs. 4 and 9. The non-relationship can be explained by the fact that physical principles of resistivity and

Table 2
The correlation geochemical - geophysical log by applying Pearson correlation. AC= acoustic wave log; CNL = Compensated neutron log; DEN=bulk density log; GR= Gamma ray log; Pe = photoelectric absorption capture section log; RD= Deep resistivity log.

Marked correlations are significant at $p < .05000$

	Al	Ca	Fe	Gd	H	Si	S	Ti	K	Th	U	AC	CNL	DEN	GR	Pe	RD
Al	1.00	0.15	**0.99**	−0.43	−0.01	**−0.80**	−0.12	**0.70**	−0.15	−0.17	0.05	0.16	−0.05	0.06	−0.16	0.03	0.14
Ca		1.00	0.17	0.03	0.01	**−0.62**	−0.10	−0.05	−0.25	−0.20	−0.02	0.06	0.21	0.21	−0.24	0.27	−0.11
Fe			1.00	−0.42	0.00	**−0.81**	−0.14	**0.67**	−0.16	−0.18	0.07	0.14	−0.04	0.07	−0.17	0.05	0.14
Gd				1.00	0.11	0.31	−0.15	−0.28	0.00	0.06	−0.01	−0.19	0.09	−0.03	0.02	0.00	−0.10
H					1.00	−0.16	−0.03	−0.07	0.14	0.15	0.17	−0.09	−0.22	−0.09	0.18	−0.11	−0.02
Si						1.00	0.16	**−0.50**	0.24	0.26	−0.04	−0.14	−0.07	−0.16	0.25	−0.19	−0.06
S							1.00	−0.06	−0.04	0.04	0.07	−0.10	−0.01	0.04	−0.02	0.01	0.02
Ti								1.00	−0.05	−0.09	−0.02	0.25	−0.07	0.05	−0.07	0.02	0.12
K									1.00	**0.81**	−0.23	−0.03	**−0.91**	**−0.83**	**0.94**	**−0.88**	0.11
Th										1.00	−0.16	−0.00	**−0.84**	**−0.69**	**0.90**	**−0.82**	0.13
U											1.00	−0.07	0.05	0.02	−0.02	0.02	−0.04
AC												1.00	0.08	0.11	−0.04	0.02	−0.12
CNL													1.00	**0.81**	**−0.93**	**0.91**	−0.19
DEN														1.00	**−0.84**	**0.88**	−0.01
GR															1.00	**−0.91**	0.10
Pe																1.00	−0.12
RD																	1.00

acoustic tools are not significantly influenced by the chemical composition of the main rock types (Pechnig et al., 2005). A negative relationship was observed with the combination of K, and Th versus CNL, DEN and Pe respectively (Table 2, and Figs. 4 & 9). These are probably related to the atomic weight of K and Th in the formation, which impact the CNL and Density logging signatures (Pechnig et al., 2005).

In situ chemical element-mineral relationships

In this research it is supposed that the factors extracted by FA may be connected to the minerals that make up the rock in CCSD-MH (4390–5089 m). FA was carried out using a correlation matrix on the standardized values of the geochemical logs that is having a zero mean and variance of 1.

We note that Ca, Gd, H, S and U were found with low communality (less than 0.4); the factor model was not fitting well including them. Based on this they were discarded from the model. The input logs studied were Fe, Al, K, Si, Th and Ti. Table 3 shows the eigenvalues, percent of total variance and cumulative variance percent explained by FA. Kaiser's criterion was applied to determine the number of factors to extract. The scree test (Cattell, 1966) in Fig. 10 can also offer a very reliable and consistent suggestion of the number of factors to extract. From Table 3, we can see that the first two factors explain approximately 76.261% of total variance. The original set of 6 logs has thus been reduced to a small set of 2 factors which accounts for 76.261% of the variance of the initial set. Table 4 shows the factor loading using Varimax(Kaiser,1958). In Table 4, F1 describes 57.515% of the total variance with high loadings of Si, Al, Fe, and Ti in between 0.84 - 0.97. This indicates that these logs show good agreement with F1. Al and Fe display the highest loads with F1. Amphibole minerals have been observed in many gneiss samples from CCSD-MH (Zhang et al., 2006). The chemical composition of Hornblende contains Ti, Fe, Si, and Al. So F1 may reflect amphibole mineral.

F2 explained 18.746% of variance with high loading of K and Th. As mentioned by Yong and Sean (2013), a factor including two variables is supposed to be reliable if the variables are strongly interrelated with each another ($r > 0.70$) but uncorrelated with other variables. Based on aforementioned we can confidently say that K and Th are reliable since they show a high correlation value of 0.81 with one another. However each showed weak correlation values with Al, Fe, Si, and Ti respectively (see Table 2). The potassium content of metamorphic rocks is derives mainly feldspar±quartz. High feldspar and quartz content of gneiss made them to have distinctive high GR value (Salim et al., 2008). The study area is underlain mainly by gneiss associated with large K-feldspar (Zhang et al., 2003, 1996). K-feldspar is generally an abundance of K and Th (Bigelow 1992). Therefore, F2 can probably be referred to as K-feldspar mineral. Konaté et al.(2017) reached a similar conclusion when inspecting the Principal Component Analysis log response at depth 100 to 2010 m from CCSD-MH.

Conclusions

Based on the study of the analysis of elemental concentration log data from the CCSD-MH (4390–5089 m) the following conclusions could be drawn:

- Cross plot is an effective way to visualize in situ elemental concentration log data. The results show that K and Th logs are the most discriminating logs followed by Al, Ti, Fe, Si, and Gd logs.
- Correlation between in situ geochemical logs and geophysical logs show that K and Th are the largest contributors to the gamma ray responses. There is no significant correlation between CNL and H. Resistivity and acoustic logs display no significant relationship with any of the in situ chemical logs .A negative relationship was observed with the combination of K, and Th versus CNL, DEN and Pe respectively.

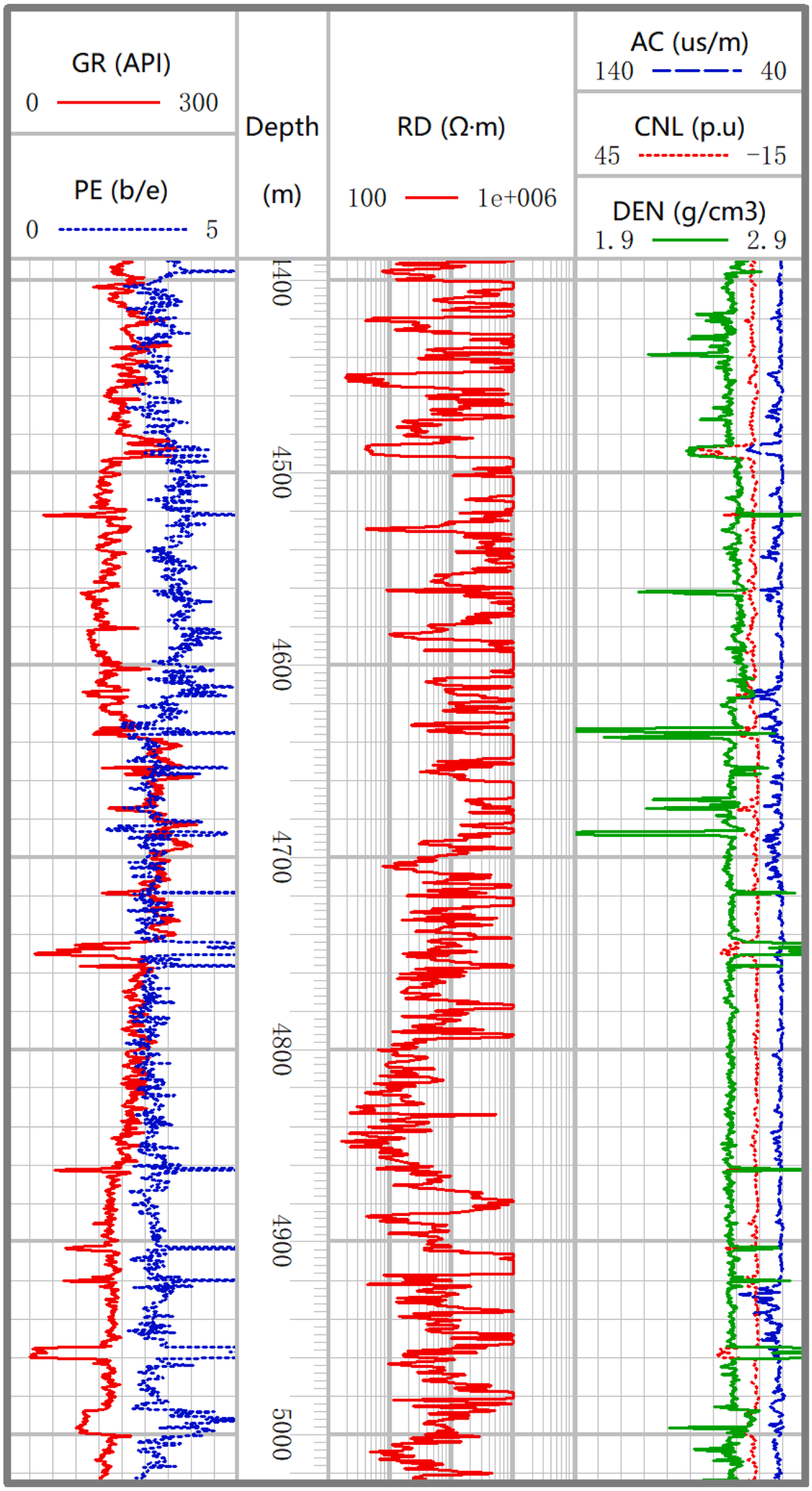

Fig. 9. The geophysical logs profile of the CCSD-MH (4390–5089 m).

Table 3
Eigenvalues, percent of total variance and cumulative variance percent explained by factor analysis. Extraction method: Principal components method was used to extract factors. Marked zone is indicating factors with eigenvalues >1. This criterion was proposed by Kaiser (1960).

Factor	Eigenvalues	% Total variance	Cumulative%
1	3.459	57.515	57.515
2	**1.125**	**18.746**	**76.261**
3	0.789	13.059	89.320
4	0.439	1.313	96.633
5	0.183	3.057	99.689
6	0.019	0.311	100

- FA is a good method to condense and interpret data concerning geochemical logging data. FA was applied using principal component extraction method and the Varimax orthogonal rotation method to the in situ elemental concentration logs in an area of UHPM rock. The results show a 2 factor model-where factor 1 (amphibole mineral) and factor 2 (K-feldspar mineral) described 76.261% of the variation in log responses. The model explained the constituent minerals that make up the rock and contribute to the characterization of rocks in the case of CCSD-MH.

Table 4
Percentage of factor loading obtained via Factor analysis. Varimax rotation (Kaiser, 1958) was applied to keeps factors uncorrelated while increasing the interpretability and utility of the factors.

Well log data	Varimax rotated result Factor1 (F1)	Factor2 (F2)
Al	**0.963**	−0.114
Fe	**0.974**	−0.107
Si	**−0.852**	0.106
Ti	**−0.843**	−0.087
K	−0.048	**0.798**
Th	−0.130	**0.751**
% variance	57.515	18.746

Declaration of Competing Interest

All authors listed have contributed sufficiently to the work to be included as authors, and all those who are qualified to be authors are

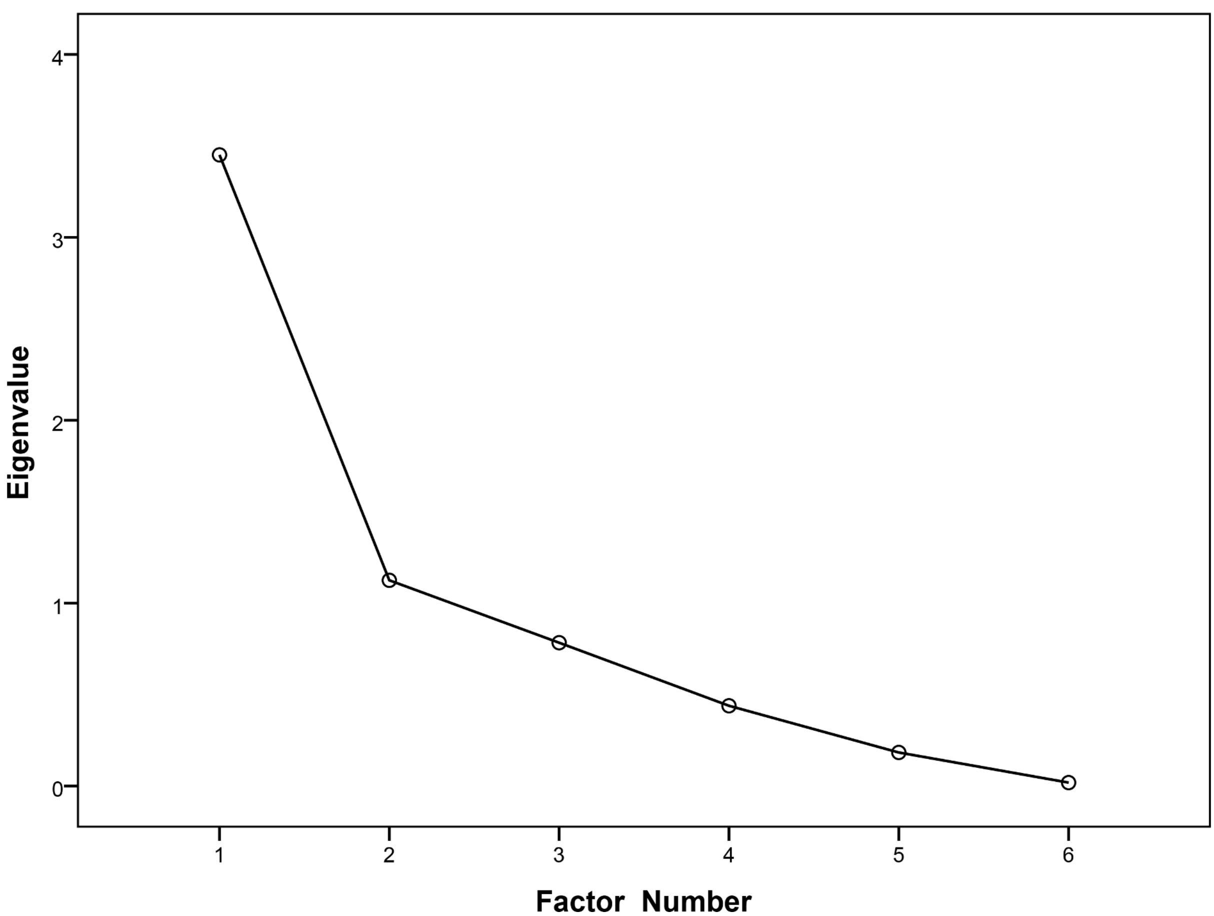

Fig. 10. The scree test of geochemical logs. The scree plot helps to determine the optimal number of factors. The eigenvalue of each factor in the initial solution is plotted in decreasing order. One then selects the index of the last factor before the plot flattens. Cattell (1966) suggested looking for the point at which the last significant drop or break takes place scree plot representing the eigenvalues.

listed in the author byline. To the best of our knowledge, no conflict of interest exists among these parties.

References

Anderson, R.N., Dove, R.E., Broglia, C., Silver, L.T., James, E.W., Chappell, B.W., 1988. Elemental and mineralogical analyses using geochemical logs from the Cajon Pass Scientific Drill hole, California, and their preliminary comparison with core analyses. Geophys. Res. Lett. 5 (9), 969–972.

Bartetzko, A., Delius, H., Pechnig, R., 2005. Effect of compositional and structural variations on log responses of igneous and metamorphic rocks. I: mafic rocks. In: Harvey, PK, Brewer, TS, Pezard, PA, Petrov, VA (Eds.), Petrophysical Properties of Crystalline Rocks, Geological Society. Special Publications, London, pp. 255–278.

Bigelow, E.L., 1992. Introduction to Wireline Log Analysis. Western Atlas International, Houston, Texas.

Bücker, C., Shimeld, J., Hunze, S., Bruckmann, W., 2000. Data report: logging while drilling data analysis of LEG 171A, a multivariate statistical approach. In Moore, J. C., and Klaus, A (eds), proceedings of the ocean drilling program. Sci. Res. 171A, 1–29.

Bosch D., Ledo J., Queralt P. (2013) Fuzzy logic determination of lithologies from well log data: application to the KTB project data set (Germany) surveys in Geophysics, 34(4): 413–439 doi:10.1007/s10712-013-9242-2.

Cattell, R.B., 1966. The Scree test for the number of factors. Multivariate Behav Res 1 (2), 245–276. https://doi.org/10.1207/s15327906mbr0102_10.

Campos da Purificacao, C.A., Nery, G.N., 2017. Petrophysical characterization and permeability estimation using well log and core data from Namorado Oil Field, Campos Basin, Brazil. In: 15th International Congress of the Brazilian Geophysical Society, held in Rio de Janeiro, Brazil, 31 July to 3 August 2017.

Das, B., Chatterjee, R., 2018. Well log Data Analysis for Lithology and Fluid Identification in Krishna-Godavari Basin, India. Arabian J. Geosci. 11, 231–242.

Fertl, W.H., 1981. Openhole Crossplot Concepts A Powerful Technique in Well Log Analysis. J Pet Technol 33 (3), 535–549. SPE-8115-PA.

Gelfort, R., 2006. On Classification of Logging Data. PhD. Thesis. Clausthal University of Technology Germany.

Gogoi, T., Chatterjee, R., 2020. Multi-mineral modeling and estimation of brittleness index of shaly sand in upper assam and mizoram areas, India, SPE reservoir evaluation and engineering-formation evaluation. SPE Res Eval & Eng. 23 (02), 708–721. https://doi.org/10.2118/200498-PA. Paper Number: SPE-200498-PA.

Ji, S.C., Xu, Z.Q., 2009. Drilling deep into the ultrahigh pressure (UHP) metamorphic terrane. Tectonophysics 475, 201–203.

Hertzog, R., Colson, L., Seeman, O'Brien, M., Scott, H., McKeon, D., Herron, M., 1989. Geochemical logging with spectrometry tools. Soc. Petrol. Eng. https://doi.org/10.2118/16792-PA.

He, L., Hu, S., Huang, S., Yang, W., Wang, J., Yuan, Y., Yang, S., 2008. Heat flow study at the Chinese Continental Scientific Drilling site: borehole temperature, thermal conductivity, and radiogenic heat production. J. Geophys. Res. 113, B02404. https://doi.org/10.1029/2007JB004958.

Herron, M.M., 1986. Mineralogy from geochemical well logging. Clays Clay Miner 34 (2), 204–213. https://doi.org/10.1346/CCMN.1986.0340211.

Kaiser, H.F., 1958. the varimax criteria for analytical rotation in factor analysis. Psychometrika 23 (3), 187–200.

Kaiser, H.F., 1960. The application of electronic computers to factor analysis. Educ. Psychol. Meas. 20, 141–151. https://doi.org/10.1177/001316446002000116.

Konaté, A.A., Pan, H., Ma, H., Cao, X., Ziggah, Y.Y., Oloo, M., Khan, N., 2015a. Application of dimensionality reduction technique to improve geophysical log data classification performance in crystalline rocks. J. Petrol. Sci. Eng. 133, 633–645.

Konaté, A.A., Pan, H.P., Fang, S.N., 2015b. Capability of self-organizing map neural network in geophysical log data classification: case study from the CCSD-MH. J. Appl. Geophys. 118, 37–46.

Konaté, A.A., Ma, H., Pan, H., et al., 2017. Lithology and mineralogy recognition from geochemical logging tool data using multivariate statistical analysis. Appl. Radiat. Isotopes 128 (1), 55–67, 2017.

Luo, M., Pan, H.P., 2010. Well logging responses of UHP metamorphic rocks from CCSD Main Hole in Sulu Terrane, Eastern Central China. J. Earth Sci. 21 (3), 347–357. https://doi.org/10.1007/s12583-010-0098-9.

Luo, M., Pan, H.P., 2011. Resistivity logs of the chinese continental scientific drilling main hole: implication for the crustal electrical structure of Dabie-Sulu Terrane, Central-Eastern China. J. Earth Sci. 22 (2), 292–298. https://doi.org/10.1007/s12583-011-0182-9.

Liu, F., Xu, Z., Yang, J., Zhang, Z., Xue, H., Meng, F., Li, T., 2005. Geochemical characteristics and genetic mechanism of orthgneiss and paragneiss in the depth intervals of 2000-3000m from main drill hole of Chinese Continental Scientific Drilling Project. Acta Petrol. Sin. 2005-02.

Liu, Q., Zeng, Q., Zheng, J., Yang, T., Qiu, N., Liu, Z., Luo, Y., Jin, Z., 2010. Magnetic properties of serpentinized garnet peridotites from the CCSD main hole in the Sulu ultrahigh-pressure metamorphic belt, eastern China. J. Geophys. Res 115, B06104. https://doi.org/10.1029/2009JB000814.

Mattsson, H., 2007. Forsmark site investigation, Interpretation of geophysical borehole measurements from KFM12A, report SKB P-07-129. Svensk Kärnbränslehantering AB.

Maiti, S., Tiwari, R.K., Kumpel, H.J., 2007. Neural network modelling and classification of litho-facies using well log data: a case study from KTB borehole site. Geophys. J. Int. 169, 733–746. https://doi.org/10.1111/j.1365-246X.2007.03342.x.

Maiti, S., Tiwari, R.K., 2009. A hybrid Monte Carlo method based artificial neural networks approach for rock boundaries identification: a case study from KTB Borehole. Pure Appl. Geophys. 166, 2059–2090. https://doi.org/10.1007/s00024-009-0533-y.

Monier-Williams M.E., Davis R.K., Paillet F.L., et al. (2009) Review of Borehole Based Geophysical Site Evaluation Tools and Techniques. NWMO TR-2009-25.

Pearson, K., 1896. Mathematical contributions to the theory of evolution. III. Regression, Heredity and Panmixia". Philos. Trans. R. Soc. London 187, 253–318. https://doi.org/10.1098/rsta.1896.0007.

Pan, H.P., Niu, Y.X., Wang, W.X., 2005. Radioactive Logging Application in CCSD Main Hole. Earth Science. J. China Univ. Geosci. 30 (Suppl), 49–56 (in Chinese with English Abstract).

Pan, H., Niu, Y., Wang, W., et al., 2006. Joint interpretation of reflectors via well logging and seismic data in the pilot hole of CCSD. Diqiu Kexue - Zhongguo Dizhi Daxue Xuebao/Earth Science. J. China Univ. Geosci. 31 (4), 569–574.

Pan, H.P., Luo, M., Zhao, Y.G., 2010. Identification of Metamorphic Rocks in the CCSD Main Hole. In: IEEE Sixth International Conference on Natural Computation (ICNC), pp. 4049–4051.

Pechnig, R., Delius, H., Bartetzko, A., 2005. Effect of compositional variations on log responses of igneous and metamorphic rocks. II: Acid and intermediate rocks. In: Harvey, P.K., Brewer, T.S., Pezard, P.A., Petrov, V.A. (Eds.), Petrophysical Properties of Crystalline Rocks, Geological Society. Special Publications, London, pp. 279–300.

Rencher, A.C., 2002. Methods of Multivariate Analysis, 2nd edition. Wiley.

Rafik, B., Kamel, B., 2016. Prediction of permeability and porosity from well log data using the nonparametric regression with multivariate analysis and neural network, Hassi R'Mel Field, Algeria, Egypt. J. Petrol. (2016) https://doi.org/10.1016/j.ejpe.2016.10.013.

Serra, O., 1984. Fundamentals of Well-Log Interpretation, 1. Elsevier, Amsterdam.

Salim, A.M.A., Pan, H.P., Luo, M., Zhou, F., 2008. Integrated log interpretation in the Chinese continental scientific drilling main hole (Eastern China): lithology and mineralization. J. Appl. Sci. 8, 3593–3602.

Szabo, N.P., 2011. Shale volume estimation based on the factor analysis of well-logging data. Acta Geophys. 59, 935.

Saggaf, M.M., Nebrija, 2000. Estimation of lithologies and depositional facies fromwireline logs. Am. Assoc. Pet. Geol. Bull. 84, 1633–1646.

Tamaki, K., Suyehiro, K., Allan, J., McWilliams, M., et al., 1992. Proceedings of the ocean drilling program. Sci. Res. Vol. 127/128 (Pt. 2).

Thurstone, L.L., 1931. The Measurement of Social Attitudes. J. Abnorm. Soc. Psychol. 26, 249–269.

Xu, Z.Q., Yang, W.C., Ji, S.C., Zhang, Z.M., Yang, J.S., Wang, Q., Tang, Z.M., 2009. Deep root of a continent–continent collision belt: evidence from the Chinese Continental Scientific Drilling (CCSD) deep borehole in the Sulu ultrahigh-pressure (HP–UHP) metamorphic terrane, China. Tectonophysics 475, 204–219.

Xu, Z.Q., Wang, Q., Tang, Z., Chen, F., 2009b. Fabric kinematics of the ultrahigh-pressure metamorphic rocks from the main borehole of the Chinese Continental Scientific Drilling Project: implications for continental subduction and exhumation. Tectonophysics 475, 235–250.

Xu, S., Okay, A.I., Ji, S., Sengor, A.M.C., Su, W., Liu, Y., Jiang, L., 1992. Diamond from the Dabie Shan metamorphic rocks and its implication for tectonic setting. Science 256, 80–82.

Yang, W.C., Liu, G., Yang, K., Cheng, Z., 2006. All-laid-out three dimensional seismic survey at the Chinese Continental Scientific Drilling site (in Chinese with English abstract). Chin. J. Geophys. 49 (3), 735–744.

Yang, H., Pan, H., Wu, A., Lu, M., 2017. Application of well logs integration and wavelet transform to improve fracture zones detection in metamorphic rocks. J. Petrol. Sci. Eng. 157, 716–723.

Yang, H., Pan, H., Ma, H., Konaté, A.A., 2016. Performance of the synergetic wavelet transform and modified K means clustering in lithology classification using nuclear log. J. Petrol. Sci. Eng. 144, 1–9.

Yang, W.C., 2009. The crust and upper mantle of the Sulu UHPM belt. Tectonophysics 475, 226–234.

Zhang, Z., Xiao, Y., Hoefs, J., Liou, J.G., Simon, K., 2006. Ultrahigh pressure metamorphic rocks from the Chinese Continental Scientific Drilling Project: I. Petrology and geochemistry of the main hole (0–2,050m). Contrib. Mineral. Petrol. 152, 421–441. https://doi.org/10.1007/s00410-006-0120-5.

Zhang, Z., Xu, Z., Xu, 2003. petrology of the non mafic UHP metamorphic rocks from a drillhole in the southern Sulu orogenic belt, eastern central China. Acta Geol. Sin. 77 (2), 173–186.

Zhang, Z., You, Z., Han, Y., 1996. Petrology, metamorphic process and genesis of the Dabi-Sulu eclogite belt, eastern –central China. Acta Geol. Sin. 9, 134–156.